# Anomalous electronic conductance in quasicrystals

Stephan Roche
*Department of Applied Physics, University of Tokyo, 7-3-1 Hongo, Bunkyo-ku, Tokyo 113-8654, Japan*

Konstantinos Moulopoulos
*Department of Natural Sciences, University of Cyprus, P.O. Box 20537, 1678 Nicosia, Cyprus*
(Received 26 July 1999)

Subtle quantum interference effects in one-dimensional quasicrystals are reported. Quite opposite to their metallic counterparts, quasiperiodic systems are shown to exhibit interesting variations of their conducting properties upon disruption of their long-range order. A sudden phason change in the structure leads to a series of transitions that proceed from extremely simple and regular to highly complex self-similar resistive patterns.

## I. INTRODUCTION

In spite of intense and continuous effort, the understanding of the exotic electronic properties of quasicrystals[1] remains unsatisfactory, although quasicrystalline materials have already been used in miscellaneous concrete applications.[2,3] The role of quasiperiodic order on electronic transport and localization is revealed by unexpected experimental findings, in both model and real quasiperiodic systems, but so far no coherent theoretical framework has been achieved.[4–7] By way of an example, one of the most distinctive features of quasicrystals is the enhancement of their conducting ability upon increase of static (structural disorder) or dynamic excitations (phonons). This has been strongly supported by a wealth of experimental evidence[4] and has often been characterized in the literature as a novel property. From a theoretical point of view, heuristic arguments[5,8] and numerical investigations [such as the ones on the Landauer conductance for quasiperiodic Penrose lattices[9] and on Kubo formula for three-dimensional (3D)-quasiperiodic models[10]] lead to a rather incomplete understanding of the observed properties which range from anomalously metallic behaviors to insulating ones.[11]

It is generally argued that a specific ''geometric localization process'' takes place in quasicrystals (maintained by critical states[12,13]) and that local disruptions of the corresponding mesoscopic order reduce the relevant quantum interferences, resulting in an increase of conductivity. Pioneer works of M. Kohmoto[12] on multifractal properties of critical states in 1D-quasiperiodic chains have been recently followed by renewed focus on the relation between localization features of such states and their ability to conduct electric current.[14] The variety of critical states discussed in the literature does not resolve questions on the relation between localization properties and transport ability. Moreover, the effect of disorder on top of these states is an even more complicated problem on which very scarce rigorous results are available. This issue has been addressed in the context of 1D quasiperiodic potentials, for which tight-binding (TB) as well as continuous Krönig-Penney models have led to simple treatments of quantum transport in the presence of a particular phason-type disorder.[15] Furthermore, attempts to rigorously establish analytical results in high-dimensional quasiperiodic systems have been facing limitations despite interesting early results.[16]

In what follows, we review, clarify, and elaborate further on exact results carried out in 1D imperfect quasiperiodic systems with a specific type of phason disorder. We find interesting variations of transmission properties that are the result of quantum interference in the presence of a sudden phason change in the quasiperiodic structure.

Section II discusses an exact treatment of a 1D quasiperiodic chain with phason disorder in a TB context. The results show that the transmission behavior undergoes strong quasiperiodic fluctuations with system size. Section III reviews and elaborates on the exact treatment of a richer system, namely a continuous quasiperiodic chain, by placing appropriate emphasis on ways to better represent its multifractal electronic properties. We find subtle interference effects of phason disorder that lead to transmission properties that were missed in the TB treatment. A qualitative phase diagram with a series of transitions is drawn, and Sec. IV presents our conclusions.

## II. INTEREFERENCE EFFECTS IN 1D QUASIPERIODIC SYSTEMS WITH DISORDER

Introduction of disorder could be typically made through randomizing of site or hopping energies (in a TB context), with the subsequent occurence of Anderson localization in the infinite chain limit. For finite systems, localization lengths may be much larger than the system size, so that conductance fluctuations as a function of energy of tunneling electrons (from the leads to the system) retain their self-similar character and still follow a power-law behavior with respect to the system size, even upon introduction of disorder as much as 10% of the total bandwith.[17] Alternatively, the particular order present in a system with long-range quasiperiodicity suggests the possible presence of unique types of defects, known as phason defects. Their geometric definition and properties have been subjected to many studies,[18] although some aspects remain controversial. It seems natural to consider how such types of defects, inherent to these systems and viewed as disruptions of quasiperiodic order, will

 

generically reduce or improve transport properties, and under what conditions this may happen. It is the aim of this work to contribute to such a more general and fundamental understanding of electronic transport properties in quasicrystals.

For 1D-quasiperiodic systems, the simplest phason defect that could be considered is of a step form in the hyperspace construction of the quasicrystal, something that amounts to a local ''patching'' of two different quasiperiodic chains. In an earlier study, such phason-defects were introduced by the authors[15] and their role on the Landauer conductance was discussed. We here review the main points in a TB context.

Tight-binding models (TBM's) of perfect quasiperiodic chains have been extensively studied both analytically and numerically for some particular values of energy, and the results have provided typical features of localization in quasiperiodic structures, such as power-law decrease of wave functions or power-law bounded resistances.[12] However, in spite of leading to interesting analytical results, TBM's do not permit the investigation of energy-dependent properties of quantum dynamics and electronic transport. The works of Kollar and Süto,[19] and Baake, Joseph, and Kramer[20] pointed out the limitations of TBM, and a manifestation of this was shown[15] in the consideration of effects of phason-type disorder on electronic localization and transmission. Let us recall the most common TB system,[15] the so-called off-diagonal TB Hamiltonian, namely

$$\mathcal{H}=\sum_n t_n(|n\rangle\langle n+1|+|n+1\rangle\langle n|).$$

This corresponds to vanishing site energies, and to hopping elements $t_n$ that take two possible values $t_A$ and $t_B$ (or for symbolic convenience $A$ and $B$) arranged in a Fibonacci sequence ABAABABAABAAB . . . . The Schrödinger equation in this so-called site representation then reads, in matrix language,

$$\begin{pmatrix}\psi_{n+1}\\ \psi_n\end{pmatrix}=M_n\cdot\begin{pmatrix}\psi_n\\ \psi_{n-1}\end{pmatrix}=M_n\cdot M_{n-1}\cdots M_1\cdot\begin{pmatrix}\psi_1\\ \psi_0\end{pmatrix}$$

$$\equiv P_n\cdot\begin{pmatrix}\psi_1\\ \psi_0\end{pmatrix} \qquad (1)$$

with transfer matrices

$$M_n=\begin{pmatrix}\frac{E}{t_n} & -\frac{t_{n-1}}{t_n}\\ 1 & 0\end{pmatrix} \quad \text{and} \quad P_n=\prod_{i=1}^{n} M_i \qquad (2)$$

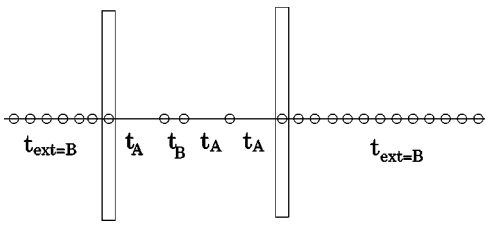


FIG. 1. Chain $N=4$: ABAA connected with perfect leads.

and with $\psi_n$ denoting the value of the wave function for energy $E$ at site $n$.

The Fibonacci arrangement of the hopping elements can be described in closed form by[21] $t_n=f(\theta_n)$ where $\theta_n$ is a kind of phase given by $\theta_n=n/\tau+\theta_0(mod1)$, with $\tau$ the golden mean [$\tau=(\sqrt{5}+1)/2$]. For the usual Fibonacci chain we have $\theta_0=0$ and then

$$f(\theta)=t_A \ \text{ for } \ 1/\tau^2\leqslant\theta<1, =t_B \ \text{ for } \ 0\leqslant\theta<1/\tau^2.$$

The quasiperiodic chain corresponding to an initial phase $\theta_0=m/\tau$ is associated with the Fibonacci sequence starting at the $m$th site of the usual one. (It should be noted here that, by changing the initial phase $\theta_0$ randomly between 0 and 1, statistical studies of the localization and transport properties of Fibonacci chains have been performed).[21,22] The particular phason-defect studied in this work is an abrupt geometric transition between two chains, one with $\theta_0=0$, and one with $\theta_0=2/\tau$. This breaks the long-range quasiperiodic order of the usual Fibonacci chain, and can be viewed as a kind of disorder, the consequences of which are reviewed below.

To study the transmission problem through such a chain with $N$ hopping elements, we imagine connecting our finite system on the left and on the right with leads, represented by periodic chains of period $t_B$ (hence $t_N=t_0=t_{ext}=t_B$) [see Fig. 1 where a small chain with five sites (four hopping elements) is shown]. But in order to avoid surface effects we must take particular care about having a system size such that the connection with $t_B$ on its right end looks like a continuation of the Fibonacci order. It is easy to see that this leads to restrictions on the possible values of the system size $N$. For both cases of Fibonacci chains with $\theta=0$ and $\theta=2/\tau$, the allowed values are $N(i=1,2,3,4\ldots)=4,12,17,25,33,38,46,51,59,\ldots$, where the integer $i$ counts the permitted possibilities and will be important in the following discussion. [Note that the difference between two consecutive allowed numbers follows a Fibonacci sequence of the numbers 8 and 5 (8,5,8,8,5,8,5,8 . . . ).]

I: $(B)$**ABAABABAABAABAB**AABABAABAABABAABAABABAA$(B)\,\theta_0=0$,

II: $(B)$AABABAABAABABAA**BABAABAABABAABAABABAABA**$(B)\,\theta_0=2/\tau$,

III: $(B)$ABAABABAABAABA**BB**ABAABAABABAABAABABAABA$(B)$.

The construction of a phason is illustrated above for a $N=29$ chain (where the phason defect has been introduced at the 16th element). Defining $\gamma=t_A/t_B$, the transfer matrix can be evaluated analytically and from this the Landauer resistances can be obtained. (Recall that the Landauer resistance of a finite chain $N$ and for fermions with spin 1/2 is given by $\rho_N=(h/2e^2)(R/T)$ where $T$ is the fraction of tunneling electrons transmitted from the system to the right lead, and $R$ is the reflected one). For a tight-binding model and for $E=0$ the resistance is related to the total transfer-matrix elements by $\rho_N=\frac{1}{4}[P_N^2(1,1)+P_N^2(1,2)+P_N^2(2,1)+P_N^2(2,2)-2]$ [for real matrix $P$, and in units of $h/2e^2$)]. For simplicity we give here the results only for $E=0$. Defining the matrices $\mathcal{A},\mathcal{B},\mathcal{C}$ by

$$\mathcal{A}=\begin{pmatrix} 0 & -\frac{1}{\gamma} \\ \gamma & 0 \end{pmatrix} \quad \mathcal{B}=\begin{pmatrix} \gamma & 0 \\ 0 & \frac{1}{\gamma} \end{pmatrix} \quad \mathcal{C}=\mathcal{B}\cdot\mathcal{A}=\begin{pmatrix} 0 & -1 \\ 1 & 0 \end{pmatrix}, \tag{3}$$

one can easily see that the product of $M_i$'s in $P_N$ appears in an inverted Fibonacci order. Moreover, noticing that $\mathcal{C}\cdot\mathcal{A}=\mathcal{C}$, $\mathcal{A}\cdot\mathcal{C}=(\mathcal{C}\cdot\mathcal{A})^{-1}$ and $\mathcal{C}^2=-1$, one shows that $P_N$ is given by $\mathcal{C}^{t(N)}\cdot\mathcal{A}^{s(N)}$, namely

$$P_N=\begin{pmatrix} 0 & -1 \\ 1 & 0 \end{pmatrix}^{t(N)} \cdot \begin{pmatrix} \gamma & 0 \\ 0 & \frac{1}{\gamma} \end{pmatrix}^{s(N)}, \tag{4}$$

where $t(N)$ and $s(N)$ are integers (dependent on $N$) which are described by a recursive relation. [For $N$ equal to a Fibonacci number $N=\{F_1,F_2,\ldots,F_{N-1},F_N\}$, Kubo and Goda [21] have investigated the statistical properties of $s(N)$ which are directly related to the characteristic exponents of self-similar wave functions; for example, by taking $(\psi_0,\psi_{-1})=(-i,1)$, it is possible to show that $|\psi_n|^2=\gamma^{-2s(N)\times(-1)^{t(N)}}$].

For the usual Fibonacci chain (called ''perfect'' in what follows) the resistance can thus be written in closed form, the result being

$$(\rho_N)_{perf}=\left(\frac{\gamma^{s(N)}-\gamma^{-s(N)}}{2}\right)^2. \tag{5}$$

The integer $s(N)$ is a fluctuating function of $N$ around zero, and its absolute value is illustrated in Fig. 2; note that it displays a self-similar pattern. Whenever $s(N_0)=0$, transmission is perfect ($T=1$). For general energies, closely related quantities to $\rho_N$ are the Lyapunov exponents (LE) $\gamma_N(E)$ for finite length systems, which provide an estimate of the dispersion of the energy spectrum. If at a given energy value, the Lyapunov exponent turns out to be nonvanishing, it means that either the corresponding states are localized, with localization length related to the inverse of the LE, or that the energy is lying in a gap.[23] LE as functions of energy are determined[24] by $\rho_N(E)=(h/2e^2)\exp[\gamma_N(E)\times N]$. Energies lying outside the spectrum are easily identified with stronger Lyapunov exponent as illustrated in Fig. 3. The

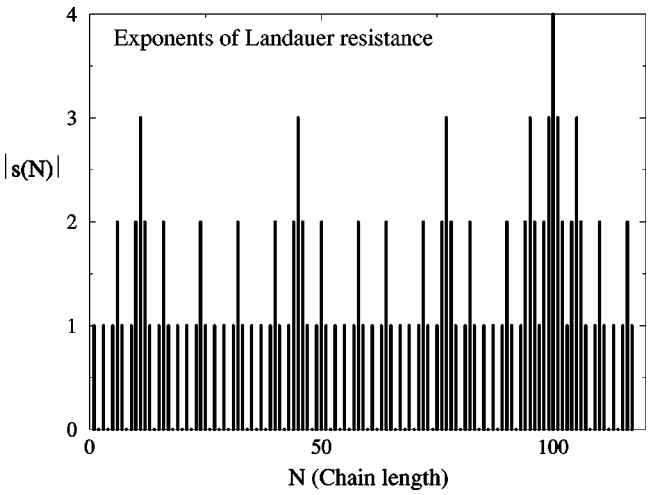


FIG. 2. Multifractal distribution of $|s(N)|$ for the Fibonacci chain of 800 sites (for $E=0$).

Cantor nature of the spectrum (characterized by zero LE) is revealed by the corresponding self-similar pattern of the distribution of finite LE zones.

After this brief review of the perfect chain, we now recall the effect of phason defect on the Landauer resistance.[15] Taking the position of the defect (denoted by $x_P$ from now on) as an internal degree of freedom, it can be shown[15] that, in this TBM, the properties of the matrices $\mathcal{A},\mathcal{B},\mathcal{C}$ are independent of $x_P$. By simple manipulations of transfer matrices, it can then be demonstrated that the total transfer matrix associated with the chain with one phason and with system size $N(i)$ is the same as the one without phason but with size $N(i+2)$. Accordingly, a general result can be written down: if $P_N$ for the perfect chain is

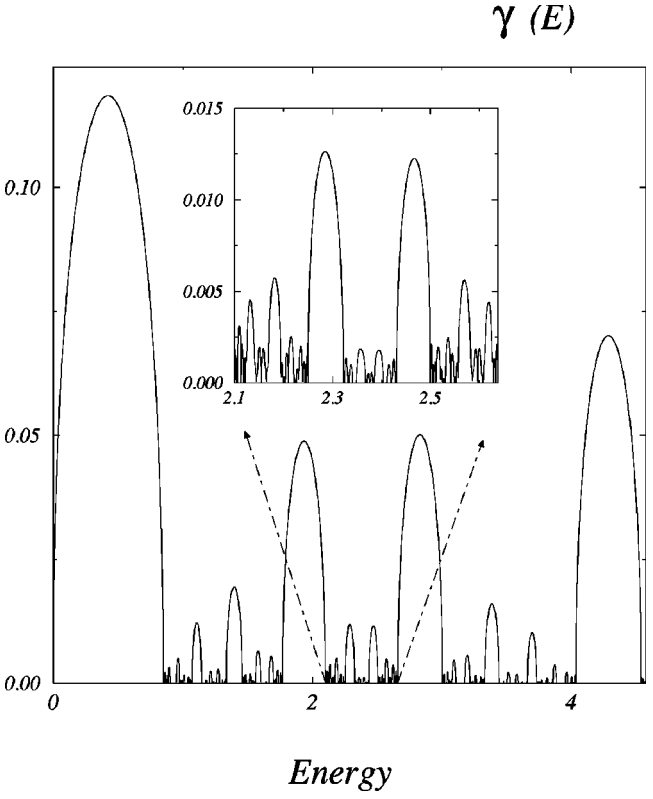


FIG. 3. Lyapunov exponents as a function of energy for a Fibonacci chain.

$$P_{N(i)}|_{perf}=\begin{pmatrix} a & b \\ c & d \end{pmatrix} \tag{6}$$

(where it is always either $a=d=0$, or $b=c=0$), then, $P_N$ for the chain with the single defect will be

$$P_{N(i)}|_{def}=P_{N(i+2)}|_{perf} = -\begin{pmatrix} 0 & -\gamma \\ 1 & 0 \end{pmatrix}\cdot\begin{pmatrix} 0 & -\frac{1}{\gamma} \\ 1 & 0 \end{pmatrix}\cdot\begin{pmatrix} a & b \\ c & d \end{pmatrix}. \tag{7}$$

The Landauer resistance of the defected system is then shown to be[15]

$$(\rho_N)_{def}=\left(\frac{\gamma^{s(N)-1}-\gamma^{-s(N)+1}}{2}\right)^2. \tag{8}$$

By comparing the resistances (5) and (8) one concludes that, at least for $E=0$, the sign of $(\rho_N)_{perf}-(\rho_N)_{def}$ is fluctuating as a function of chain length, which in turn implies that, statistically speaking, the phason defect does not alter the transport properties in the thermodynamic limit $N\to\infty$.

Finally, to determine the role of more than one phason defects, we consider the sequence constructed following the same defect type (of a step form in hyperspace) but now maximizing the number of defects allowed for each size $N$ (multiphason case). We then once again calculate analytically the Landauer resistance $\rho_N|_{mult}$. By way of illustration, for chains with $N=4$ and $N=17$, one has one possible defect of this type in the former, and four of them in the latter:

$$(B)-\mathrm{ABBA}-(B),$$

$$(B)-\mathrm{ABBABBAABABBABBAA}-(B).$$

With the same transfer matrices $\mathcal{A},\mathcal{B}$ previously introduced and by noticing that the blocks BAABAB and BAB simply lead to the matrices $\mathcal{A}$ and $-\mathcal{B}\equiv\tilde{\mathcal{B}}$, respectively, we show that the products that determine $P_N$ now follow the Fibonacci order, namely

$$P_N=\mathcal{A},\ \mathcal{A}\tilde{\mathcal{B}},\ \mathcal{A}\tilde{\mathcal{B}}\mathcal{A},\mathcal{A}\tilde{\mathcal{B}}\mathcal{A}\mathcal{A}\tilde{\mathcal{B}},\mathcal{A}\tilde{\mathcal{B}}\mathcal{A}\mathcal{A}\tilde{\mathcal{B}}\mathcal{A}\tilde{\mathcal{B}}\mathcal{A},$$

$$\mathcal{A}\tilde{\mathcal{B}}\mathcal{A}\mathcal{A}\tilde{\mathcal{B}}\mathcal{A}\tilde{\mathcal{B}}\mathcal{A}\mathcal{A}\tilde{\mathcal{B}}\mathcal{A}\mathcal{A}\tilde{\mathcal{B}},\ldots.$$

Using this, the analytical form of $\rho_N|_{mult}$ is finally shown to be

$$(\rho_N)_{mult}=\left(\frac{\gamma^{\tilde{s}(N)}-\gamma^{-\tilde{s}(N)}}{2}\right)^2 \tag{9}$$

with $\tilde{s}(N)$ a new integer function of $N$, also determined recursively. An interesting point to observe is that the function $\rho_N|_{perf}-\rho_N|_{def}$ for a single phason defect changes its sign at each step $N(i)\to N(i+1)$, whereas $\rho_N|_{perf}-\rho_N|_{mult}$ exhibits fluctuations on a much larger range. By way of an example, chains with sizes respectively equal to $N(i=1,2,3,4,5\cdots17)=5-203$ sites follow $\rho_N|_{perf}-\rho_N|_{mult}\geqslant 0$, whereas the behavior is opposite for chains with 330 to 456 sites, and so forth.

In conclusion, in this TBM and at least for $E=0$, even the highest density of phason defects does not break down the localization mechanism which does remain basically the same in the limit $N\to\infty$, and is associated to quasiperiodic fluctuations of the Landauer resistance as a function of length (in fact, these fluctuations turn out to asymptotically follow a power-law behavior in the infinite length limit). In the next section, an exact continuous model will yield results that, in fact, *do* depend on $x_P$ and that display an interesting structure. The absence of such structure in a TBM should be attributed to loss of the relevant long-range interference effects, due to truncation errors inherent to any TB approximation.

## III. LANDAUER RESISTANCE OF A KRÖNIG-PENNEY MODEL WITH PHASONS

We now discuss an exact continuous model that does not suffer from the known truncation errors of the TB approximation. In this continuous model we first review the main calculations as earlier described by the authors.[15] We then perform power-spectra calculations of the Landauer resistance interference patterns, in order to clarify the relation between localization properties and transmission ability of critical states.

In the Krönig-Penney model,[25] the potential describing the interaction of the electron with the lattice is represented by a sum of Dirac $\delta$-function potentials with intensity $V_n$ localized at $x_n$, namely $V(x)=\Sigma_n V_n\delta(x-x_n)$, the $x_n, V_n$ being chosen as either correlated or uncorrelated variables. In between two successive scattering centers, the solution of the Schrödinger equation is a linear combination of two plane waves: $\Psi(x)=A_n e^{ik(x-x_n)}+B_n e^{-ik(x-x_n)}$ $(x_n\leqslant x\leqslant x_{n+1})$, the 1D wave vector $k>0$ being related to the energy $E$ through $E=\hbar^2k^2/2m$. In the Krönig-Penney model, a solution of the problem is constructed by imposing continuity conditions for the wave function and its derivative on the scattering centers. For the sake of simplicity, we choose the case where the intensity of scattering potentials is constant $(V_n=\lambda)$, whereas the scattering centers are quasiperiodically spaced $\{(x_n-x_{n-1})\}=\{a,b\}=\{\tau,1\}$: a set of these two lengths arranged in a Fibonacci sequence. The problem can then be described by transfer matrices as follows:

$$\begin{pmatrix} A_{n+1} \\ B_{n+1} \end{pmatrix}=\Lambda(n)\cdot\begin{pmatrix} A_n \\ B_n \end{pmatrix} \tag{10}$$

with

$$\Lambda(n)=\begin{pmatrix} \left(1-\frac{i\lambda}{2k}\right)e^{ik(x_{n+1}-x_n)} & -\frac{i\lambda}{2k}e^{ik(x_{n+1}-x_n)} \\ \frac{i\lambda}{2k}e^{-ik(x_{n+1}-x_n)} & \left(1+\frac{i\lambda}{2k}\right)e^{-ik(x_{n+1}-x_n)} \end{pmatrix}. \tag{11}$$

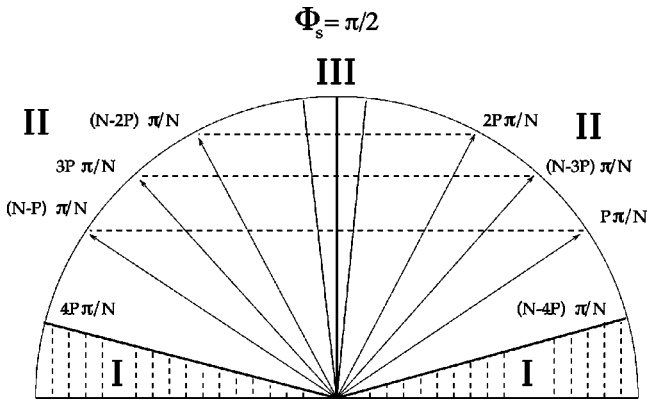


FIG. 4. Energy-dependent phase diagram.

Within this framework, it is known that the Landauer resistance of a system of size $N$ is given by $\rho_N=|P_N(1,2)|^2$, now with $P_N\equiv\Lambda(N)\cdots\Lambda(1)$. On the other hand, a renormalization group associated with the Fibonacci chain enables to map the electronic spectrum to a dynamical system defined by the traces of the transfer matrices (the well-known trace map[12]). This trace map provides a quantity (usually denoted by $I$) that remains invariant during the renormalization-group flow. In continuous models such as the one we discuss here, this quantity $I$ is energy dependent, something that is in sharp contrast to what one obtains for a TBM.[26] In our case, one finds $I(k)=\lambda^2\sin^2k(a-b)/4k^2$ whose zeros are given by $k_s=n\pi/(a-b)$, with $n$ integer. These points, referred to as conducting points, are especially interesting since they correspond to the commutation of the transfer matrices, $[P_n,P_{n+1}]=0$ given that[20]

$$4I+2=\mathrm{Tr}(P_n\cdot P_{n+1}\cdot P_n^{-1}\cdot P_{n+1}^{-1}).$$

But even more than this, the elementary matrices $\Lambda$ also commute: the general result for the commutator[15]

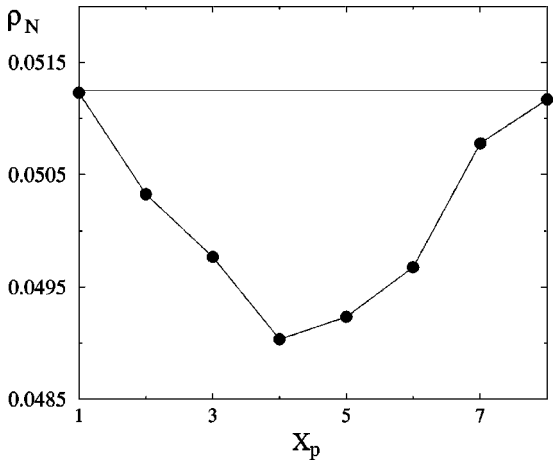


FIG. 5. Landauer resistance as a function of phason position $x_P$, for $\varepsilon=10^{-4}$, $N=33$, and $m=1$.

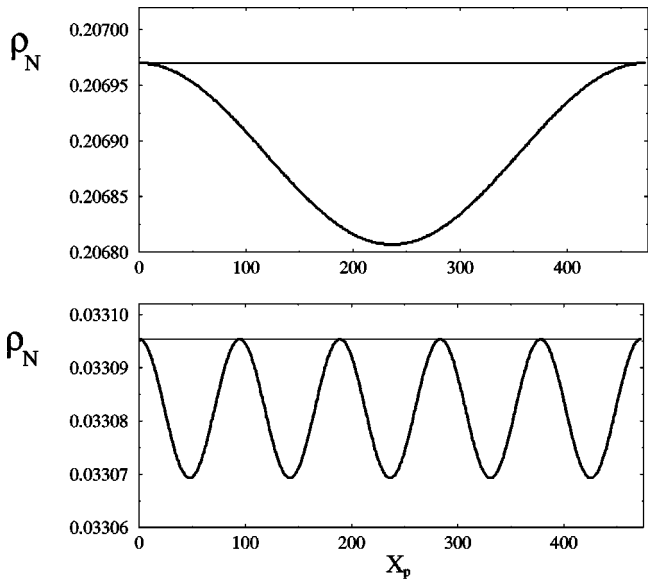


FIG. 6. Landauer resistances as a function of phason position $x_P$ $(N=2000,P=472)$ with $\varepsilon=[10^{-9},10^{-6}]$, for $m=1$ (upper curve) and $m=5$ (lower curve). For higher values of $\varepsilon$, then $\rho_N\to\infty$ which indicates that energy lies within a gap, or may be associated with a localized state.

$$[\Lambda(\Delta x=a),\Lambda(\Delta x=b)]=\lambda\frac{e^{ik(a-b)}}{4k^2}\ (1-e^{2ik(b-a)})\times\begin{pmatrix}\lambda & \lambda-2ik\\ -\lambda-2ik & -\lambda\end{pmatrix} \quad (12)$$

vanishes for $k=k_s=n\pi/(a-b)$. For such energies therefore, one can change the order of the hopping elements without affecting the transmission properties. In fact, the resistance can be written down analytically at $k_s$, namely

$$\rho_N|_{k=k_s}=\left(\frac{\lambda}{2k_s}\right)^2\frac{\sin^2N\varphi}{\sin^2\varphi}, \quad (13)$$

$\varphi$ being a phase dependent on $k_s^2$ and $\lambda$, and defined by $|\cos\varphi|=|\cos k_sa+\lambda/2k_s\sin k_sa|$, or equivalently by $|\cos\varphi|=|\cos k_sb+\lambda/2k_s\sin k_sb|$ (*both* are valid for $k=k_s$). The analytical form of $\rho_N|_{k=k_s}$ indicates that when $N\to\infty$, the Landauer resistance oscillates but remains bounded, so that the energies $k_s^2$ correspond to states that lead to best transmission (recall that localized states would display exponential increase of resistance with length). [It has also been shown[19,20] that at these points we have the highest density (a clustering) of energy eigenvalues in the infinite limit.] Following our earlier discussion,[15] we restrict our study to energies $k^2=(k_s+\varepsilon)^2$, i.e., in the vicinity of $k_s$ [hereafter $k_s=n\pi/(\tau-1)$ (i.e. $a=\tau,b=1$) is taken without loss of generality]. We then proceed with the numerical determination of $\rho_N$ with the help of appropriate products of the two basic matrices:

$$\Lambda_A=\begin{pmatrix} \left(1-\frac{i\lambda}{2k}\right)e^{ik\tau} & -\frac{i\lambda}{2k}e^{ik\tau} \\ \frac{i\lambda}{2k}e^{-ik\tau} & \left(1+\frac{i\lambda}{2k}\right)e^{-ik\tau} \end{pmatrix}$$

$$\Lambda_B=\begin{pmatrix} \left(1-\frac{i\lambda}{2k}\right)e^{ik} & -\frac{i\lambda}{2k}e^{ik} \\ \frac{i\lambda}{2k}e^{-ik} & \left(1+\frac{i\lambda}{2k}\right)e^{-ik} \end{pmatrix}. \qquad (14)$$

Then by choosing $\lambda$ so that $\rho_N|_{k=k_s}=0$ exactly at $k=k_s$ (namely enforcing a conducting behavior at these special energies, for either a perfect or a defected chain), leads to $N-1$ values for $\lambda$, given by $\lambda_s=2k_s(\cos\varphi_s-\cos k_s)/\sin k_s$ with the phase $\varphi_s$ defined by $\varphi_s=(m\pi)/N$ with $m=1,\ldots,N-1$. The $N-1$ values of $\varphi_s$ are symmetrically distributed around $\pi/2$ and cover densely the entire upper half of the trigonometric plane when increasing $N$.[15] Recalling that $x_P$ is taken as the position of phason defect (**BB**) in the chain, with $x_P\in[1,P]$ an integer and $P$ the maximum number of defect-positions for a given chain, we now summarize the main resulting patterns[15] for $\rho_N(x_P,\varphi_s,\varepsilon)$ and also present their power spectra. (It is important to emphasize that $\rho_N$ *does* depend on $x_P$ in contrast to the approximate TBM of the previous section.)

In the above results the numerical accuracy is always checked through $detP_N=1$ which determines the resolution. The Landauer resistance calculated in $k=k_s$ is always found to be $\sim 10^{-12}$–$10^{-13}$ and thus determines the numerical uncertainty on $\rho_N$. The main results for both perfect and defected chains are sketched on the phase diagram in Fig. 4, where several features can be identified. First, note that an interesting pseudosymmetry is observed around $\pi/2$ for $\rho_N(x_P,m,\varepsilon)$ which does *not* correspond to any symmetry in the scattering potential (see Figs. 4 and 5 for illustrations).

In the zones labeled as zone **I** the phason defect reduces the resistance for energies sufficiently close to the conducting points (see Figs. 5 and 6). Two symmetrical such zones are $m<N-4P$, and $m>4P$ with $\rho_N|_{perf}(x_P,m,\varepsilon)>\rho_N|_{def}(x_P,m,\varepsilon)$. In other words, for these values of parameters the Fibonacci chain becomes more conducting upon introduction of local phason. This effect is a pure result of quantum interference at zero temperature and has been shown for tunneling energies close to the ones of conducting points, being therefore representative of the behavior of electrons that contribute to the conduction mechanism. We illustrate these behaviors writing down all the eight different inequivalent defected chains for a system of 34 sites (or $N=33$):

$$FIBO{:}--B--ABAABABAABAABABAABABAABAABABAABAA--B--,$$

$$Def1{:}--B--A\mathbf{BB}ABAABAABABAABABAABAABABAABAABA--B--,$$

$$Def2{:}--B--ABAABA\mathbf{BB}AABABAABABAABAABABAABAABA--B--,$$

$$Def3{:}--B--ABAABABAA\mathbf{BB}ABAABABAABAABABAABAABA--B--,$$

$$Def4{:}--B--ABAABABAABAABA\mathbf{BB}ABAABAABABAABAABA--B--,$$

$$Def5{:}--B--ABAABABAABAABABAABA\mathbf{BB}AABABAABAABA--B--,$$

$$Def6{:}--B--ABAABABAABAABABAABABAA\mathbf{BB}ABAABAABA--B--,$$

$$Def7{:}--B--ABAABABAABAABABAABABAABAABA\mathbf{BB}AABA--B--,$$

$$Def8{:}--B--ABAABABAABAABABAABABAABAABABAA\mathbf{BB}A--B--.$$

It is interesting that, although for such a small system the resistance of the defected samples above does not follow a simple pattern as a function of the defect position $x_P$ (see Fig. 5), the resulting $\rho_N|_{def}(x_P,m,k)$ for long chains approaches a continuous limit which is given by a simple oscillatory form, namely $\rho_N|_{def}(x_P,m,k)\sim\alpha(m/P)\sin[(2m\pi/P)x_P]$. This is further illustrated in Fig. 6 for chains with $N=2000$, and $m=1,5$.

Subtleties in the relations between the spatial structure of critical states and their corresponding transport properties have been discussed recently by Maciá[14] by analyzing the power spectra of phonon modes. Here, we also display power spectra (Figs. 7 and 11–13) for the different resistance patterns, that provide a different way of exhibiting the details of the electronic interference resulting from the presence of the phason disorder.

The power spectrum of the $m=5$ resistance is given in Fig. 7, where the only eigenfrequency appearing agrees well with $m/P=5/472=0.0106$. (Superimposed small oscillations are an unphysical effect due to a Fourier transform of a finite signal.)

Let us now move to zone **II**. For $N-4P<m<4P$, the

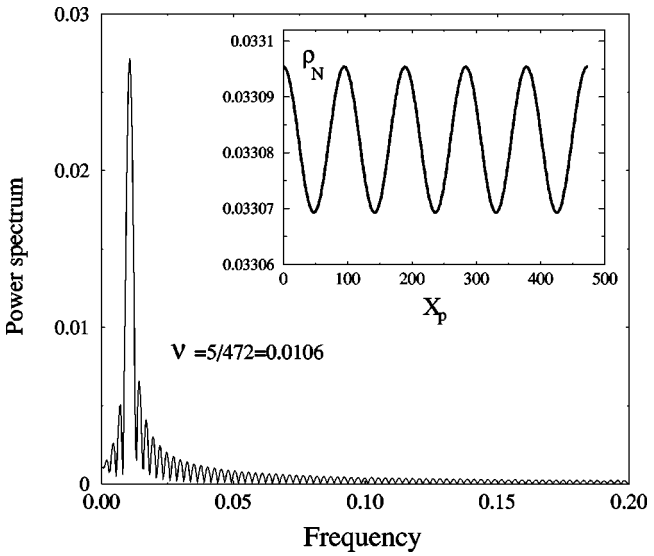


FIG. 7. Power spectrum of the pattern given in the inset for $m=5$ and same parameters as in previous figure.

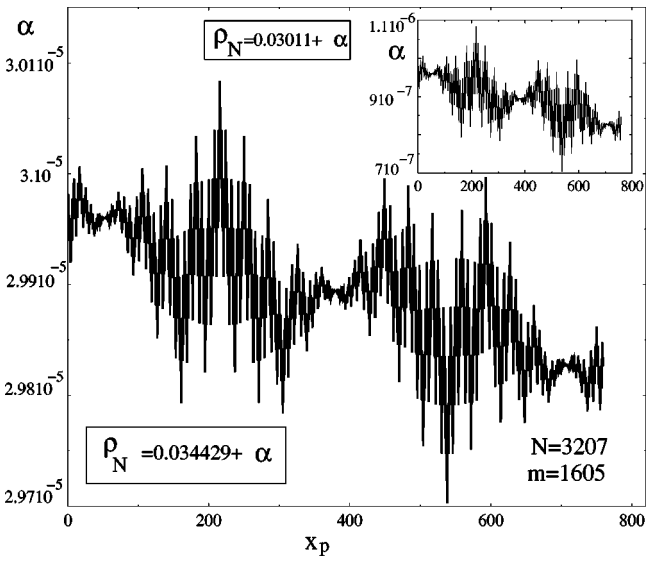


FIG. 9. Typical Landauer resistance in zone **III**, displaying self-similar patterns as described in the text.

resistance patterns become more complex but recurrent simple $(m-P)$ periodic oscillatory patterns are found around the values $\varphi_s=\{(N-4P)/N,\ (N-3P)/N,\ (N-2P)/N,\ (N-P)/N\}\pi$ and symetrically for $\tilde{\varphi}_s=\{4P/N,\ 3P/N,\ 2P/N,\ P/N\}\pi$. In these regions of parameter space, there is a genuine transition from systematic increase to decrease (and vice versa) of the electronic resistance upon introduction of local phason, as illustrated in Fig. 8.

Finally, there is a zone **III** around $\varphi\sim\pi/2$, where self-similar patterns are observed, and these suggest that $\rho_N|_{\mathrm{III}}(x_P)$ reveal critical states which are robust against phason disorder as found in the TBM case. The typical patterns represented in Fig. 9 present oscillations of the resistance where smaller oscillations seem to be superimposed by some coefficients $s(n)$ like the ones appearing in Sec. II. In Fig. 10, the case with 3000 sites is shown, with different values of the scattering potential in the vicinity of the symmetry point $\varphi=\pi/2$. (For $m=1497$, the potential is $\lambda\sim3.918$, for $m=1498$ it is $\lambda\sim3.929$, and 3.941 for $m=1499$.) The patterns exhibit only small differences with each other, and their Fourier spectrum is almost identical (see below). The power spectra of those patterns are given in Figs. 11 and 12, and they show that superimposed frequencies are identical for different values of $m$. The highest frequency is given by $\nu=0.5$ which is related to the change of $\rho_N(x_P\rightarrow x_{P+1})$ (here $x_{P+1}$ denotes the next allowed position of the defect). In corresponding figures five unambiguous frequencies have been clearly identified and named $\nu_{n=1,5}$. This indicates that

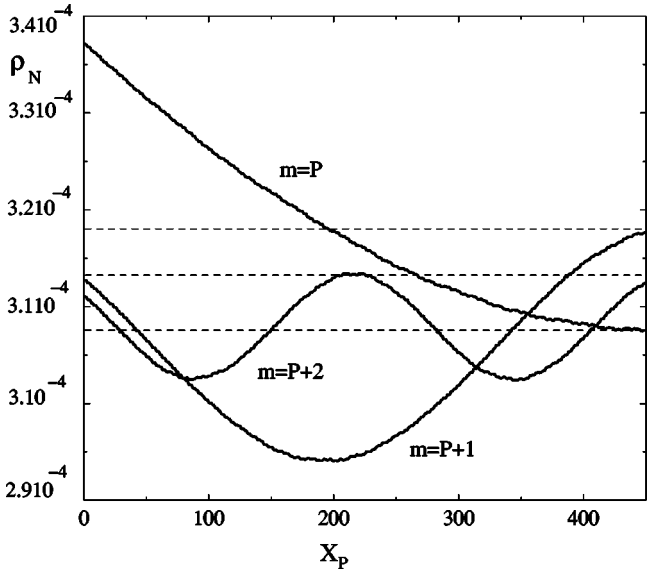


FIG. 8. Regular evolution of interference pattern for $m=P,P+1,P+2$, and $N=2000$, $P=472$. For $\varphi_s=P\pi/N$, Fibonacci chain is always less resistive than the imperfect one, whereas transitions occur for $m=P+1,P+2,\ldots$. Dashed curves are the values for Fibonacci chains with same parameter $m$ as in the corresponding imperfect one.

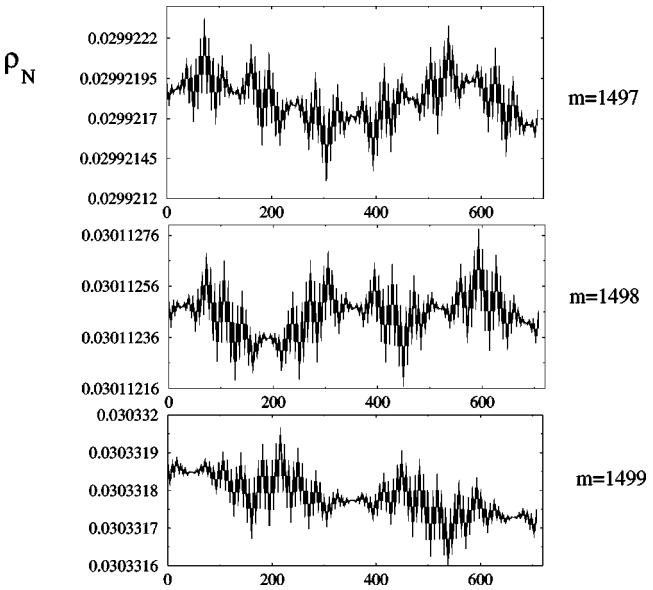


FIG. 10. Interferences pattern for several values of scattering potentials close to $\varphi\sim\pi/2$ (horizontal axis represents the defect position $x_P$).

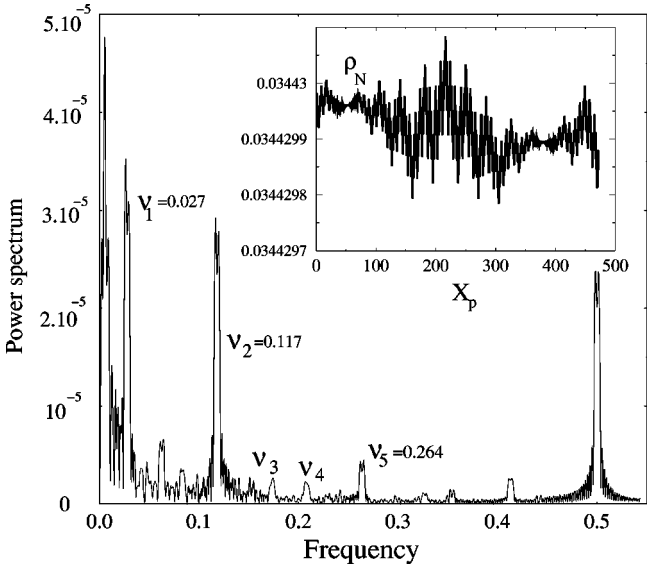


FIG. 11. Self-similar interference pattern for $N=3207$, $P=757$, and $m=1605$. Stability is ensured from $\varepsilon=10^{-3}$ down to the numerical resolution limit.

all these apparently critical patterns are in fact described by the same function, which seems to be a superposition of several independent frequencies convoluted with a function defined by a series of $s(n)$-type coefficients.

So far the analysis concerned energies very close to conducting points, and we found simple forms emerging for $\rho_N$ and its power spectra, resulting from a superposition of several frequencies. One of the interesting findings is the formation of zones **I**, **II**, **III** and the observation that the complexity of the patterns is increasing as we move through zones in ascending order (always up to the pseudosymmetry around $\varphi=\pi/2$). For larger energies we seem to get to a truly chaotic regime, where we find fluctuations such as those shown in the inset of Fig. 13. As energies get farther from conducting points $k_s=\pi/(\tau-1)$ the resistance is sharply increasing by several orders of magnitude. The power spectrum in such cases reveals many more eigenfrequencies, with the interesting emergence of frequencies with similar amplitudes labeled by $\nu$ and $\omega$ (that share some resemblance with the ''twin peaks'' introduced recently[14] for phonons, an issue that deserves further investigation). In all these cases the behaviors of the Landauer resistance of the perfect Fibonacci chain versus the imperfect one follows complicated random fluctuations.

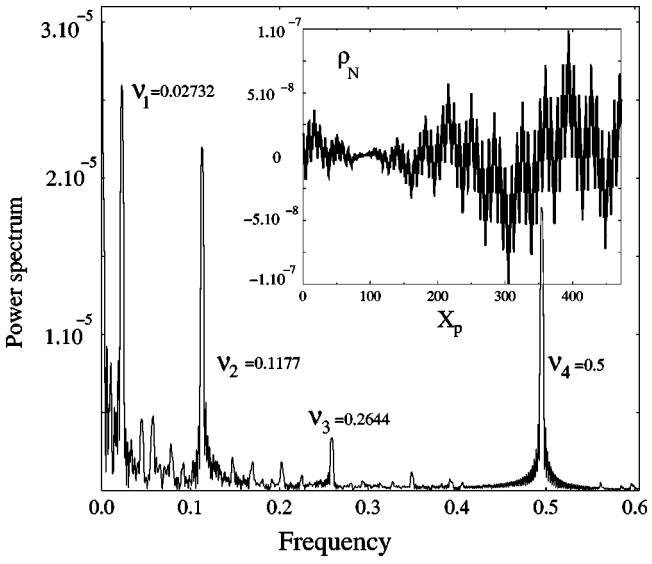


FIG. 12. Same as previous figure with different $m$.

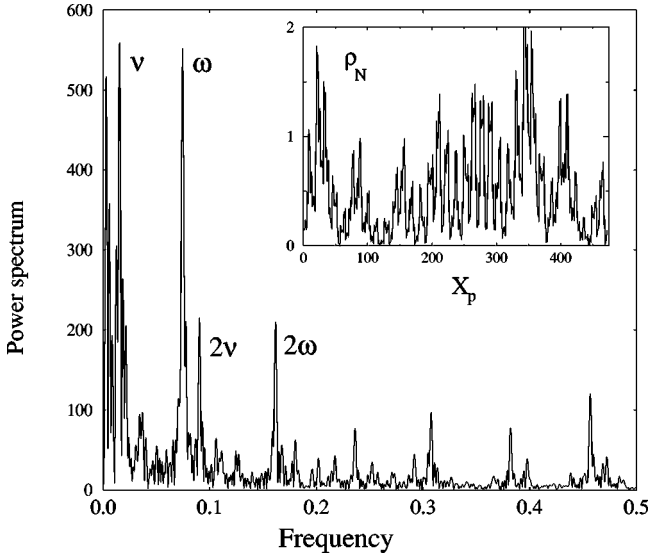


FIG. 13. Landauer resistance interference pattern for $\varepsilon=0.5$, $N=2000$, and $P=472$.

The different behaviors found in this study of the continuous model suggest that in some cases local disruption of long-range quasiperiodic order has improved the conducting ability of the chain in a systematic manner. Analyzing the interference patterns of the Landauer resistance as a function of energy and of the phason-defect position suggests that extendedness (as a localization property of available states at such energies) has also been simultaneously improved. This is manifested by a bounded and simple oscillatory pattern for the resistance, similar to what is found for extended eigenstates in periodic systems.

In conclusion of this section, several important points should be re-emphasized: our study concerned the transmission behavior around the special conducting points $k_s$, that seem to be the location of highest density of eigenenergies[19,20] and can therefore be relevant to real systems. The Krönig-Penney model has been able to unravel subtle quantum interference effects of phason disorder on localization and transmission properties that were missed in the treatment of TBM. Here following earlier results,[15] we have found that, although multiphason defects in TBM do not seem to alter the transmission ability of corresponding states, for continuous models, interesting interference patterns are revealed by $\rho_N$ as a function of the defect position and the distance from $k_s$. Furthermore their power-spectra analysis is proposed as an original way to determine how phason defects affect simultaneously localization and transport modes.

## IV. CONCLUSION

Several interesting features occurring in the electronic transport properties of 1D quasicrystals have been reported.

Quantum interferences have been shown to generate interesting resistance patterns, which are modified in even more ways by phason defects, viewed as a natural disruption of quasicrystalline order. A qualitative phase diagram has been drawn with a series of transitions that proceed from exceedingly simple and regular to highly complex self-similar resistive patterns. It is an open question whether such patterns in 1D systems may survive or partly retain their character in higher dimension.

## ACKNOWLEDGMENTS

S.R. is indebted to the European Commission for financial support (Contract No. ERBIC17CT980059), and to Professor T. Fujiwara from the Department of Applied Physics of Tokyo University for hospitality.

[1] D. Shechtman, I. Blech, D. Gratias, and J.W. Cahn, Phys. Rev. Lett. **53**, 1951 (1984).
[2] J.M. Dubois *et al.*, Ann. Chim. (Paris) **19**, 3 (1994); S. Roche, *ibid.* **23**, 953 (1998).
[3] *New Horizons in Quasicrystals: Research and Applications*, edited by A.I. Goldman, D.J. Sordelet, P.A. Thiel, and J.M. Dubois (World Scientific, Singapore, 1997).
[4] C. Berger, *Mesoscopic Quantum Physics*, edited by E. Akkermans, G. Montambaux, J.L. Pichard, and J. Zinn-Justin, Les Houches Summer School Proceedings, Vol. LXI (North-Holland, Amsterdam, 1994).
[5] S. Roche, G. Trambly de Laissardière, and D. Mayou, J. Math. Phys. **38**, 1794 (1997).
[6] T. Fujiwara, in *Physical Properties of Quasicrystals*, edited by Z.M. Stadnik, Springer Series in Solid-State Sciences Vol. 126 (Springer, New York, 1999), p. 169.
[7] S. Roche and T. Fujiwara, Phys. Rev. B **58**, 11 338 (1998).
[8] C. Sire, in it Lectures on Quasicrystals, edited by F. Hippert and D. Gratias (Les Editions de Physique Les Ulis, Paris, 1994).
[9] S. Yamamoto and T. Fujiwara, Phys. Rev. B **51**, 8841 (1995).
[10] S. Roche and D. Mayou, Phys. Rev. Lett. **79**, 2518 (1997).
[11] J. Delahaye, C. Berger, and Brisson, Phys. Rev. Lett. **81**, 4204 (1998).
[12] M. Kohmoto, L. P. Kadanoff, and Ch. Tang, Phys. Rev. Lett. **50**, 1870 (1983); **50**, 1873 (1983); M. Kohmoto, Int. J. Mod. Phys. B **1**, 31 (1986); M. Kohmoto and J.R. Banavar, Phys. Rev. B **34**, 563 (1986).
[13] E. Maciá and F. Domínguez-Adame, Phys. Rev. Lett. **76**, 2957 (1996), and references therein.
[14] E. Maciá, Phys. Rev. B **60**, 10 032 (1999).
[15] K. Moulopoulos and S. Roche, Phys. Rev. B **53**, 212 (1996).
[16] K. Moulopoulos and S. Roche, J. Phys.: Condens. Matter **7**, 8883 (1995).
[17] S. Das Sarma and X.C. Xie, Phys. Rev. B **37**, 1097 (1988).
[18] T.C. Lubensky, J.E.S. Socolar, P.J. Steinhardt, P.A. Bancel, and P.A. Heiney, Phys. Rev. Lett. **57**, 1440 (1986); G. Coddens, R. Bellissent, Y. Calvayrac, and J.P. Ambroise, Europhys. Lett. **16**, 271 (1991); A. Trub and H.R. Trebin, J. Phys. (France) **4**, 1855 (1994); H. Klein, M. Audier, M. Boudarda, M. de Boissieu, L. Beraha, and D. Duneau, Philos. Mag. A **73**, 309 (1996).
[19] J. Kollar and A. Süto, Phys. Lett. A **117**, 203 (1986).
[20] M. Baake, D. Joseph, and P. Kramer, Phys. Lett. A **168**, 199 (1992).
[21] M. Goda and H. Kubo, J. Phys. Soc. Jpn. **58**, 3624 (1989); H. Kubo and M. Goda, *ibid.* **60**, 2729 (1991); **62**, 2601 (1993).
[22] F. Wijnands, J. Phys. A **22**, 3267 (1989).
[23] A. Süto, in *Beyond Quasicrystals*, edited by F. Axel and D. Gratias (Les Editions de Physique, Paris, 1994), p. 483.
[24] E. Maciá, F. Domínguez-Adame, and A. Sanchez, Phys. Rev. B **49**, 9503 (1994), and references therein.
[25] R. de L. Krönig and W.G. Penney, reprinted in *Mathematical Physics in One Dimension: Exactly Soluble Models of Interacting Particles*, edited by E.H. Lieb and D.C. Mattis (Academic, New York, 1966), p. 243.
[26] M. Baake, U. Grimm, and D. Joseph, Int. J. Mod. Phys. B **7**, 1527 (1993).